SBGf33599

Optimization-based Reservoir Modeling: Example on a Million-cell Model

Wenceslau Peres Gouveia Jr.,A. S. Cullick,Clayton V. Deutsch

University of Alberta/ Mobil Oil Company

Abstract

3-D reservoir characterization procedures aim at achieving a spatial distribution of reservoir properties that is consistent with the available reservoir data. Geostatistical algorithms, probably the most popular approach for reservoir characterization, have indeed provided a practical methodology to this problem. These techniques, however, have been somewhat limited on the number of data sets they can account for and on the propagation of data uncertainties and data resolution on reservoir properties to the final model.

We have proposed an optimization-based approach for reservoir modeling (Gouveia *et al.*, 1998) that can overcome some of these limitations. This algorithm provides a framework to integrate a broad spectrum of data sets (well, seismic, production and geological data) in such a way that the respective degrees of data uncertainty and resolution are taken into consideration. These features come at a considerable computational cost when compared to geostatistical techniques. However, via a modified Monte Carlo sampling procedure, we were able to reduce the computational cost to the point that the proposed methodology can be applicable to more realistic reservoir modeling situations. Here, we report results that illustrate the performance of the optimization algorithm on the modeling of a synthetic reservoir parameterized by a one-million-cell model defined on a Cartesian grid.

INTRODUCTION

The assessment of exploitation alternatives relies on an accurate three-dimensional spatial description of a hydrocarbon reservoir. Such a description must be constrained by all available information about the reservoir, which incorporates a broad spectrum of data sets -geological, geophysical and engineering data- that have different resolution and distinct levels of uncertainty. Each data component offers constraints at different levels on one or more reservoir parameters. For instance, seismic data are informative on the structure of the reservoir layers and on the spatial distribution of lithofacies and porosity. Production data constrain the reservoir permeability and, to some degree, the spatial distribution of lithofacies (Wen *et. al*, 1998). Those constraints have to be fully accounted for in a reservoir characterization procedure. Moreover, the reservoir model must reflect the conceptual geological model that is associated with the depositional environment under consideration.

In Gouveia *et al.* (1998) we have extended the optimization-based approach for reservoir modeling initiated by Deutsch (1992) to allow the integration of a larger number of data sets in such a way that data uncertainty and data resolution are taken into consideration. The approach leads to three objective functions –one for lithofacies, one for porosity and one for permeability- which minimization results in models that are by construction consistent with the available reservoir information. These objective functions consist of a summation of a number of components, each build to account for a specific data type. Due to the non-differentiable nature of some of their components, we had to resort to derivative-free optimization methods, specifically simulated annealing. The optimization procedure starts by assigning to a randomly selected cell of an initial reservoir model a new lithofacies or property value. Once the objective function is re-evaluated, the new model is accepted or not according to standard simulated-annealing rules. The process is then repeated until a given convergence criterion is met. We were able to reduce the well-known high computational cost of such a Monte-Carlo approach by devising mechanisms for fast evaluation of the objective function -some of them described in Deutsch (1992)- and by modifying the model-updating scheme used in the optimization. Instead of randomly assigning a new value to a selected reservoir cell, we use some of the available reservoir data to build a local probability density function (PDF) from which the updated cell value is drawn. Such a more elaborated model-updating scheme results in a faster convergence of the optimization.

Enhancements such as these improved the computational performance of the optimization algorithm to the point it can be used in larger reservoir modeling problems. Here, we report results obtained when we applied the proposed approach to the characterization of lithofacies, porosity and permeability of a reservoir parameterized by one million cells defined on a Cartesian grid.

THE RESERVOIR DATA

We based our study on a segment extracted from a model of a Mobil producing reservoir, which has a shallow-marine depositional origin. The model contains six lithofacies: a shale lithofacies and five reservoir facies. Table 1 summarizes the reservoir data used in the modeling. All data components have been computed from the "true" reservoir model, as it will be detailed next. In addition to the data listed in the table, we have used 25 well log profiles that were extracted from the "true" model and used as "well data."

Spatial Modeling	***Data Input***
Lithofacies	1. Variograms 2. Depth proportions 3. Seismic-scale proportions 4. Transition probabilities
Porosity	1. Seismic-scale porosity 2. Facies-dependent porosity histograms
Permeability	1. Production-scale permeability 2. Facies-dependent porosity-permeability cross plots

Table1: Data used in the reservoir characterization

LITHOFACIES DATA

We have determined indicator variograms and depth-dependent proportions for each of the six lithofacies using the "true" exhaustive reservoir model. Adding to these data, we have assumed that sand and shale seismic-scale proportions (volume content) are available from seismic data. These were obtained by calculating the proportions of seismic sand and shale lithofacies from the "true" model for the entire depth interval of the reservoir. Thus, the seismic data do not provide any vertical resolution on the vertical distribution of lithofacies. In this example, the sand seismic lithofacies includes all reservoir lithofacies, and the seismic shale lithofacies is equivalent to the reservoir shale lithofacies. Such a relationship between seismic and reservoir lithofacies is relevant to the characterization procedure and has to be defined prior to the reservoir modeling. To account for uncertainties in the seismic estimates of lithofacies, the seismic information is incorporated into the modeling procedure not as single numbers but as local PDFs. Both the coarser scale constraint provided by the seismic data as well as the local PDFs can be accounted for by the optimization procedure as detailed in Gouveia *et al.* (1998).

The last lithofacies data component considered in the modeling are the so-called transition probabilities. An n^{th}-order transition probability quantifies the probability of a given configuration of lithofacies in *n* successive grid cells along a pre-specified direction. These quantities are one possible way to incorporate more detailed geological depositional information, when compared to 2^{nd}-order statistics such as variograms. Here, we have considered 4^{th}-order transition probabilities along three directions: North-South, East-West and along the main dip of the reservoir.

POROSITY DATA

The seismic-scale porosity information used in the porosity modeling was computed by averaging the porosity of the "true" reservoir model across its depth interval. As in the seismic-lithofacies situation, there is the assumption that the seismic data only provide areal resolution. Again, we have used local PDFs as a mechanism to account for the uncertainty associated with the porosity estimates in the final reservoir model. In addition to the seismic-scale porosity information, we have used facies-dependent porosity PDFs to impose the appropriate porosity variability on each of the reservoir lithofacies.

PERMEABILITY DATA

Inversion of flowing well pressure data to spatial permeability fields is an active area of research in reservoir engineering. We assume that such information is available to constrain the spatial distribution of reservoir permeabilities. In this study, the "production-data" derived permeability field was in fact obtained by averaging (upscaling) the "true" permeability reservoir model to result in a two-dimensional spatial description of permeability over the reservoir area. As in the case with seismic data, we assumed that the production data did not provide resolution across the depth interval of the reservoir. Moreover, along the same lines as before, we have assigned local PDFs to the upscaled permeability in order to incorporate the uncertainty associated with the production-data-inversion procedure. Those PDFs are then used as constraints for the spatial distribution of the finer-scale reservoir permeabilities (Gouveia *et al.* , 1998). In conjunction with the coarse scale permeability information, we have used facies dependent porosity-permeability cross-plots which are informative on the variance of permeability within pre-specified porosity ranges for each one of the lithofacies. Next we present the reservoir models obtained from the optimization algorithm when we used the information summarized in this section as constraints on the spatial distribution of lithofacies and properties. We also show some diagnostics that quantify the extent to which the "optimum" reservoir models are consistent with the input reservoir data.

RESERVOIR LITHOFACIES AND PROPERTY MODELING

The objective functions for lithofacies, porosity and permeability consist of a weighted sum of components, each one measuring the misfit between the reservoir model and a specific input data sets (Gouveia *et al.* , 1998),

$$O[f_r,\phi_r,\kappa_r] \quad = \quad \sum_{i=1}^{N_c}\frac{1}{w_i}\| Q_i[data_i]-Q_i[reservoir]\|,$$

where f_r,ϕ_r and κ_r represent the lithofacies, porosity and permeability distributions, respectively. N_c is the number of objective function components and w_i its respective standard deviation. The operator $Q[\bullet]$ maps an input data set into a specific constraint (e.g., a variogram model), that is to be applied to the reservoir model via the optimization.

Optimization of the lithofacies objective function results in the model illustrated in Figure 1. The initial model is not fully random, rather it is consistent with the seismic-scale shale proportions. The convergence of the objective function is shown in Figure 2 for 10^7 iterations, what amounts to 10 iterations per reservoir cell. The behavior of each one of the components is illustrative of the non-linearity of this optimization problem. To speed up the convergence rate we have used the transition probabilities to assign a new lithofacies value for a selected reservoir cell in the course of optimization. Due to space limitations, we will show only a few diagnostics that demonstrate the extent to which the model illustrated in Figure 1 honors the available lithofacies reservoir data. Figure 3 is a combined plot that shows the input seismic shale proportions and the seismic-scale shale proportions of the optimum model. Figure 4 shows the fit of the North-South transition probabilities associated with this model to the ones computed from the true model. The component related to the depth lithofacies proportions presents the slowest convergence among all components. Notice that the initial and final values of the seismic objective function component are similar, what is related to the fact that the initial model of the optimization is already consistent with the seismic data information.

The porosity objective function was reduced to a final normalized misfit level of 0.09 after 10^6 iterations. The optimum porosity model is illustrated in Figure 5. Figure 6 shows that the trends of the seismic-scale porosity distribution associated with the optimum model is in good agreement with the ones present in the “seismic”-derived porosity information. Here, the approach to update the porosity at a reservoir cell was based on the facies-specific porosity histograms.

Finally, the optimization of the permeability objective function achieved a reduction of 90% of the initial value of the objective function after 10^6 iterations. The optimum permeability model is illustrated in Figure 7. Finally, the model-updating scheme used in the permeability optimization resorted to the conditional porosity-permeability PDFs.

CONCLUSIONS

We have presented an application of an optimization-based methodology for reservoir modeling on a synthetic data set. The reservoir model, parameterized by 10^6 cells on a Cartesian grid, was subject to a number of data-derived constraints. In principle, the proposed methodology is able to accommodate differences in terms of resolution and uncertainty associated with the input data sets. Although this flexibility comes at a considerable cost, when compared to geostatistical formulations, we were able to accelerate the convergence of the optimization algorithm via simple enhancements on the model-updating scheme.

ACKNOWLEDGEMENTS

We thank Mobil Oil Corporation for permission to present this work.

REFERENCES

Deutsch, C.V., 1992, Annealing techniques applied to reservoir modeling and the integration of geological and engineering well test data, Ph.D. thesis, Stanford University.

Deutsch, C.V., 1997, Direct assessment of accuracy and precision: 5th Internat. Geostatistics Congress, Wollongong, Australia.

Gouveia, W.P., Cullick, A.S., and Deutsch, C.V., 1998, An optimization framework for reservoir characterization: 68th Annual Internat. Mtg. Soc. Expl. Geophys., Expanded Abstracts, 1830-1842.

Wen, X.H., Cullick, A.S., Deutsch, C.V., and Gouveia, W.P., 1999, Facies proportions maps from multiple well production data, Submitted to In Situ.

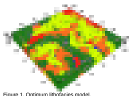

Figure 1. Optimum lithofacies model.

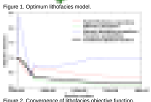

Figure 2. Convergence of lithofacies objective function.

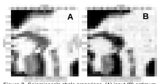

Figure 3. Seismicscale shale proporions. (A) input (B) optimum model.

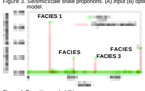

Figure 4. Transition probabilities.

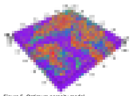

Figure 5. Optimum porosity model.

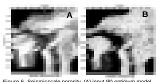

Figure 6. Seismicscale porosity. (A) input (B) optimum model.

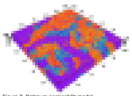

Figure 7. Optimum permeabilitymodel.